Electronic Supplementary Material (ESI) for Physical Chemistry Chemical Physics.

Supporting Information: Prediction of Anisotropic NMR Data without Knowledge of Alignment Medium Structure by Surface Decomposition

Yizhou Liu,[a]* Ikenna E. Ndukwe,[b,c] Mikhail Reibarkh,[b] Gary E. Martin,[b,d] R. Thomas Williamson[b,e]

a. Analytical Research and Development, Pfizer Worldwide Research and Development, 445 Eastern Point Road, Groton, CT, 06340, USA. Email: Yizhou.Liu@pfizer.com

b. Analytical Research and Development, Merck & Co. Inc., 126 E. Lincoln Ave., Rahway, NJ, USA 07065.

c. Current address: Pivotal Attribute Sciences, Amgen Inc., One Amgen Center DriveDrive, Thousand Oaks,Oaks, CA 91320.

d. Current address: Seton Hall University, Department of Chemistry and Biochemistry, 400 South Orange Ave., South Orange, NJ 07079.

e. Current address: University of North Carolina at Wilmington, Department of Chemistry and Biochemistry, 5600 Marvin K. Moss Lane, Wilmington, NC 28409.

Table of Contents

List of Tables

Supplementary theory

Orientational distribution function of a solute in the liquid crystal

Equations in the SI are referred to as Eq S(i) and equations in the main text are referred to Eq (i). For a LC system of *N* identical mesogens and one solute, the system partition function is given by:

$$Z = \frac{Z_k}{N!h^{6(N+1)}} \int dr \int da \prod_{i=1}^{N} \left(\int dr_i \int da_i \right) \prod_{j=1}^{N} exp\left[-\beta\, U(a,r,a_j,r_j) \right] \prod_{k,l=1(k>l)}^{N} exp\left[-\beta\, U(a_k,r_k,a_l,r_l) \right] \qquad S(1)$$

Part of the partition function associated with kinetic energy (covering the momentum and angular momentum degrees of freedom) is not written out but labeled as Z_k. h is the Planck constant. The position and orientation of the solute in the laboratory-frame are described by r and a, respectively, and the position and orientation of each mesogen in the laboratory-frame is described by subscripted r and a, respectively. $\int dr \int da \prod_{i=1}^{N} \left(\int dr_i \int da_i \right)$ is the multiple integral over all positional and orientational degrees of freedom. $\prod_{j=1}^{N} exp\left[-\beta\, U(a,r,a_j,r_j) \right]$ in the integrand is the Boltzmann factor associated with pairwise interaction of the solute with *N* mesogens, and $\prod_{k,l=1(k>l)}^{N} exp\left[-\beta\, U(a_k,r_k,a_l,r_l) \right]$ in the integrand is the Boltzmann factor associated with pairwise interactions between the *N* mesogens ($k > l$ to avoid double counting).

Next, we consider the subsystem of the *N* mesogens and assume that the positional and orientational distribution of these mesogens is not affected by the solute. Then the probability density of finding the subsystem at a particular microstate described by $a_1,r_1,a_2,r_2,\cdots,a_N,r_N$ is given by:

$$P(a_1,r_1,a_2,r_2,\cdots\cdots,a_N,r_N) = \frac{\prod_{k,l=1(k>l)}^{N} exp\left[-\beta\, U(a_k,r_k,a_l,r_l) \right]}{\prod_{i=1}^{N} \left(\int dr_i \int da_i \right) \prod_{k,l=1(k>l)}^{N} exp\left[-\beta\, U(a_k,r_k,a_l,r_l) \right]} \qquad S(2)$$

The denominator is the partition function of the subsystem potential energy (integrated over positional and orientational degrees of freedom), and will be denoted by $Z_p^{'}$ in the following. Eq S(1) can then be rewritten as:

$$Z = \frac{Z_k\, Z_p^{'}}{N!h^{6(N+1)}} \int dr \int da \prod_{i=1}^{N} \left(\int dr_i \int da_i \right) \prod_{j=1}^{N} exp\left[-\beta\, U(a,r,a_j,r_j) \right] P(a_1,r_1,a_2,r_2,\cdots,a_N,r_N) \qquad S(3)$$

The mean-field approximation is applied next, by which each mesogen moves and rotates independently in an average field produced by all the other mesogens, yielding the approximation:

$$P(a_1,r_1,a_2,r_2,\cdots,a_N,r_N) \approx P(a_1,r_1)\, P(a_2,r_2) \cdots P(a_N,r_N) \qquad S(4)$$

Substituting Eq S(4) into Eq S(3) and factoring Z into products of N pairwise solute-mesogen interactions leads to:

$$Z \approx \frac{Z_k Z_p^{'}}{N! h^{6(N+1)}} \int dr \int da \left\{ \int dr_m \int da_m P(a_m, r_m) \, exp\left[-\beta \, U(a,r,a_m,r_m) \right] \right\}^N \qquad S(5)$$

Here, r_m and a_m represent the position and orientation of a mesogen. Note that $P(a_m, r_m)$ is the same for all mesogens so integration over position and orientation leads to the same result for all pairwise interactions, which is raised to the power of N in Eq S(5).

From Eq S(5), we can calculate the probability density of finding the solute at position r and a by:

$$P_s(a,r) \approx \frac{\left\{ \int dr_m \int da_m P(a_m, r_m) \, exp\left[-\beta \, U(a,r,a_m,r_m) \right] \right\}^N}{\int dr \int da \left\{ \int dr_m \int da_m P(a_m, r_m) \, exp\left[-\beta \, U(a,r,a_m,r_m) \right] \right\}^N} \qquad S(6)$$

Because the solution is spatially homogenous, r and a are independent variables such that $P_s(a,r)$ is related to the orientational distribution function of the solute $f_s(a)$ by:

$$P_s(a,r) = \frac{f_s(a)}{V} \qquad S(7)$$

$V = \int dr$ is the sample volume. Likewise, for the mesogen we have:

$$P(a_m, r_m) = \frac{f_m(a_m)}{V} \qquad S(8)$$

A homogenous solution also implies that the pairwise potential only depends on the relative position between the solute and the mesogen. If we now use r to represent the relative position (note that the same variable label was used earlier for the solute position), and substitute Eq S(7) and S(8) into Eq S(6), we obtain:

$$f_s(a) \approx \frac{\left\{ \int dr \int da_m f_m(a_m) \, exp\left[-\beta \, U(a,r,a_m) \right] \right\}^N}{\int da \left\{ \int dr \int da_m f_m(a_m) \, exp\left[-\beta \, U(a,r,a_m) \right] \right\}^N} \qquad S(9)$$

If we restrict our discussion to steric (hard-body) interaction only ($U = U^{HB}$) and define the average excluded volume $\langle V_{ex}(a) \rangle$ by Eq (2), we can obtain Eq (1). Note that besides $\langle V_{ex}(a) \rangle$, we can also define the average accessible volume as:

$$\langle V_a(a) \rangle = \int dr \int da_m f_m(a_m) \, exp\left[-\beta \, U(a,r,a_m) \right] \qquad S(10)$$

Obviously, $\langle V_{ex}(a) \rangle + \langle V_a(a) \rangle = V$. The solute ODF can also be expressed as:

$$f_s(a) \approx \frac{\langle V_a(a)\rangle^N}{\int da\, \langle V_a(a)\rangle^N} \qquad S(11)$$

Dilute LLC approximation and order transfer equation

Dividing both the numerator and denominator in Eq S(1) in the main text by V^N leads to:

$$f_s(a) \approx \frac{\left[1 - \frac{\langle V_{ex}(a)\rangle}{V}\right]^N}{\int da \left[1 - \frac{\langle V_{ex}(a)\rangle}{V}\right]^N} \qquad S(12)$$

Binomial expansion of the numerator gives:

$$\left[1 - \frac{\langle V_{ex}(a)\rangle}{V}\right]^N = \sum_{n=0}^{N} \binom{N}{n} \left[-\frac{\langle V_{ex}(a)\rangle}{V}\right]^n \qquad S(13)$$

The dilute LLC approximation truncates the expansion after $n > 1$, which leads to the greatly simplified order transfer equation Eq (6). To better understand terms ignored in this approximation, here we will consider the general structure of the order transfer equation (OTE) for an arbitrary order n. The basic idea is to express the left side of Eq S(13) as a multipole expansion on the basis of spherical harmonic functions of the solute orientation a, *i.e.*, as below:

$$\left[1 - \frac{\langle V_{ex}(a)\rangle}{V}\right]^N = \sum_l \sum_m Y_l^m(a) \langle \bar{Y}_l^m \rangle_S \qquad S(14)$$

, where $\langle \bar{Y}_l^m \rangle_S$ is directly related to the solute order parameters. Towards this objective, we start by multipole expansion for $f_m(\hat{R}\, a)$ in Eq (5), yielding:

$$\langle V_{ex}(a)\rangle = \sum_l \sum_m Y_l^m(a) \sum_{m'} \left\langle \bar{Y}_l^{m'} \right\rangle_M \int d\boldsymbol{\Omega} \left[D^{\,l}_{m\,m'}(\hat{R}) \right]^* \int dr \left\{ 1 - exp\left[-\beta U^{HB}(\boldsymbol{\Omega}, r) \right] \right\} \qquad S(15)$$

The orientational relationship between the solute and the mesogen is described by Figure 1 in the main text. The bar over $\bar{Y}_l^{m'}$ denotes complex conjugate. $\left\langle \bar{Y}_l^{m'} \right\rangle_M$ represents mesogen order parameters. As the expression will soon get rather lengthy, we simplify notation by defining a function:

$$g^{\,l}_{m\,m'} = \frac{1}{V} \int d\boldsymbol{\Omega} \left[D^{\,l}_{m\,m'}(\hat{R}) \right]^* \int dr \left\{ 1 - exp\left[-\beta U^{HB}(\boldsymbol{\Omega}, r) \right] \right\} \qquad S(16)$$

The value of $g^{\,l}_{m\,m'}$ is on the order of $\frac{\langle V_{ex}(a)\rangle}{V}$, thus an extremely small pure number independent of a (as mentioned in the main text, the dilute LLC approximations implies even $Ng^{\,l}_{m\,m'}$ is much smaller than 1 ($Ng^{\,l}_{m\,m'} \ll 1$)). With this short-hand notation, Eq S(13) becomes:

$$\left[1-\frac{\langle V_{ex}(a)\rangle}{V}\right]^N=\sum_{n=0}^{N}(-1)^n\binom{N}{n}\left[\sum_l\sum_m Y_l^m(a)\sum_{m'}\left\langle \bar{Y}_l^{m'}\right\rangle_M g_{m'm}^{l}\right]^n \qquad S(17)$$

Expanding the multiple summation on the left side of Eq S(17) by power n generates a series of products between spherical harmonic functions of a, and converting these products stepwise into the total angular momentum basis leads to the following expression for $\langle \bar{Y}_l^m\rangle_S$:

$$8\pi^2\langle \bar{Y}_l^m\rangle_S = -\binom{N}{1}\sum_{m'}\left\langle \bar{Y}_l^{m'}\right\rangle_M g_{m'm}^{l}$$

$$+\binom{N}{2}\sum_{l_1}\sum_{m_1}\sum_{m_1'}\sum_{l_2}\sum_{m_2}\sum_{m_2'}\left\langle \bar{Y}_{l_1}^{m_1'}\right\rangle_M\left\langle \bar{Y}_{l_2}^{m_2'}\right\rangle_M g_{m_1'm_1}^{l_1} g_{m_2'm_2}^{l_2} h(l_1,m_1,l_2,m_2,l,m)$$

$$-\binom{N}{3}\sum_{l_1}\sum_{m_1}\sum_{m_1'}\sum_{l_2}\sum_{m_2}\sum_{m_2'}\sum_{l_3}\sum_{m_3}\sum_{m_3'}\left\langle \bar{Y}_{l_1}^{m_1'}\right\rangle_M\left\langle \bar{Y}_{l_2}^{m_2'}\right\rangle_M\left\langle \bar{Y}_{l_3}^{m_3'}\right\rangle_M g_{m_1'm_1}^{l_1} g_{m_2'm_2}^{l_2} g_{m_3'm_3}^{l_3}\sum_{L_1}\sum_{M_1} h(l_1,m_1,l_2,m_2,L_1,M_1)h(L_1,M_1,l_3,m_3,l,m)$$

$$+\sum_{n\geq 4}^{N}(-1)^n\binom{N}{n}\sum_{l_1}\sum_{m_1}\sum_{m_1'}\sum_{l_2}\sum_{m_2}\sum_{m_2'}\cdots\sum_{l_n}\sum_{m_n}\sum_{m_n'}\left\langle \bar{Y}_{l_1}^{m_1'}\right\rangle_M\left\langle \bar{Y}_{l_2}^{m_2'}\right\rangle_M\cdots\left\langle \bar{Y}_{l_n}^{m_n'}\right\rangle_M g_{m_1'm_1}^{l_1} g_{m_2'm_2}^{l_2}\cdots g_{m_n'm_n}^{l_n}$$

$$\sum_{L_1}\sum_{M_1}\cdots\sum_{L_{n-2}}\sum_{M_{n-2}} h(l_1,m_1,l_2,m_2,L_1,M_1)\cdots h(L_{n-2},M_{n-2},l_n,m_n,l,m) \qquad S(18)$$

The function h is a short-hand notation representing the projection coefficient of the direct product basis onto the total angular momentum basis, given by:

$$h(l_a,m_a,l_b,m_b,l_c,m_c)=(-1)^{m_c}\sqrt{\frac{(2l_a+1)(2l_b+1)(2l_c+1)}{4\pi}}\begin{pmatrix} l_a & l_b & l_c\\ 0 & 0 & 0\end{pmatrix}\begin{pmatrix} l_a & l_b & l_c\\ m_a & m_b & -m_c\end{pmatrix} \qquad S(19)$$

The 2x3 array inside the parenthesis represents the Wigner 3*j*-symbols.

Eq S(18) is the mesogen-to-solute OTE for up to any power of n. Note that axisymmetric order is not assumed here. Term associated with the combination factor $\binom{N}{n}$ is the contribution due to the *n*-th order. In Eq S(18), we listed $n=1,2,3$ terms on the first three lines, respectively, followed by the general expression for higher orders. The dilute LLC approximation only retains the $n=1$ term. Contributions from higher order terms diminish when the LLC concentration is low, mainly because $\binom{N}{n}g_{m_1'm_1}^{l_1} g_{m_2'm_2}^{l_2}\cdots g_{m_n'm_n}^{l_n}$ decreases sharply as n goes up ($Ng_{m'm}^{l}\ll 1$). Note that most of the order parameter product terms $\left\langle \bar{Y}_{l_1}^{m_1'}\right\rangle_M\left\langle \bar{Y}_{l_2}^{m_2'}\right\rangle_M\cdots\left\langle \bar{Y}_{l_n}^{m_n'}\right\rangle_M$ are also very small except when all but one l's are zero, in which case the truncation of these terms is rationalized by their product with the very small $\binom{N}{n}g_{m_1'm_1}^{l_1} g_{m_2'm_2}^{l_2}\cdots g_{m_n'm_n}^{l_n}$ as just mentioned.

When only the $n=1$ term is retained, we can obtain the following OTE after some straightforward calculation:

$$\langle \bar{Y}_l^m \rangle_S \approx \sum_{m'} \langle Y_l^{m'} \rangle_M \left\{ \frac{N}{8\pi^2 V} \int d\boldsymbol{\Omega} \left[D_{m'm}^{l}(\hat{R}) \right]^* \int dr \exp\left[-\beta U^{HB}(\boldsymbol{\Omega}, r) \right] \right\} \qquad S(20)$$

After taking the complex conjugates of both sides, we obtain Eq (6). In this work, we refer to $\langle Y_l^m \rangle_S$ *in lieu* of their conjugates as order parameters, which is valid as long as this change is reflected in the calculation of NMR parameters, *e.g.*, in this work, the conversion to Saupe ordering matrix is adjusted for $\langle Y_l^m \rangle_S$ (refer to Eq (7)).

Finally, we provide the expanded expression for V_{ex}^r in Eq (3). Substituting Eq (5) into Eq (3) followed by multipole expansion of $f_m(\hat{R}\, a)$ leads to:

$$V_{ex}^r = \frac{1}{8\pi^2} \int da \sum_l \sum_m Y_l^m(a) \sum_{m'} \langle Y_l^{m'} \rangle_M \int d\boldsymbol{\Omega} \left[D_{m'm}^{l}(\hat{R}) \right]^* \int dr \left\{ 1 - exp\left[-\beta U^{HB}(\boldsymbol{\Omega}, r) \right] \right\} \qquad S(21)$$

Because integrating $Y_l^m(a)$ over a is zero when $l > 0$, only the $l = 0$ term survives, yielding:

$$V_{ex}^r = \frac{1}{8\pi^2} \int d\boldsymbol{\Omega} \int dr \left\{ 1 - exp\left[-\beta U^{HB}(\boldsymbol{\Omega}, r) \right] \right\} \qquad S(22)$$

Note that Eq S(22) and Eq (5) only differ in that the integration over $\boldsymbol{\Omega}$ is weighted by the mesogen ODF f_m in Eq (5) whereas in Eq S(22) all orientations are equally weighted by an isotropic factor $\frac{1}{8\pi^2}$ as if the molecules are randomly rotating around each other.

Orientation order of a landscape on the mesogen

As mentioned in the main text, two ODFs can be defined for a representative landscape (LS_{rep}) residing on the MEB-ES of a mesogen: f being the ODF wrt the laboratory frame and f' being the ODF wrt a fixed mesogen frame. The mesogen also has an ODF defined wrt the laboratory frame: f_m. From the standpoint of surface parametrization for NMR prediction, order parameters associated with the laboratory frame ODF (f) of the LS_{rep} are the direct targets of parametrization. However, a relationship clearly should exist between f, f', and f_m, which is interesting to look at and potentially useful in some applications.

For this purpose, we can still refer to the orientational relationships depicted in Figure 1 in the main text. Here, the blue frame represents the mesogen whose laboratory-frame orientation is described by the uniaxial director a_m, and the green frame represents a LS_{rep} whose orientation is related to the blue frame through a rotation operator $\hat{R}$ by Euler angles α, β, and γ. The position of the director in the LS_{rep} (green) frame is denoted by a. Because the probability of finding the mesogen at orientation $\hat{R}a$ in the laboratory frame is $d\boldsymbol{\Omega}\, f_m(\hat{R}\, a)$ and the probability density of the LS_{rep} being oriented wrt the mesogen frame by $\hat{R}$ is $f'(\hat{R})$, the probability density of finding the LS_{rep} at orientation a in the laboratory frame is given by:

$$f(a) = \int d\boldsymbol{\Omega}\, f_m(\hat{R}\, a)\, f'(\hat{R}) \qquad S(23)$$

Multipole expansion for $f(a)$ and $f_m(\hat{R}\,a)$ on both sides and equating the coefficients for $Y_l^m(a)$ gives:

$$\langle \bar{Y}_l^m \rangle_L = \sum_{m'} \langle \bar{Y}_l^{m'} \rangle_M \langle [D^{\,l}_{m'm}]^* \rangle_L \qquad S(24)$$

, where:

$$\langle [D^{\,l}_{m'm}]^* \rangle_L = \int d\boldsymbol{\Omega}\ f^*(\hat{R}) \left[D^{\,l}_{m'm}(\hat{R})\right]^* \qquad S(25)$$

$\langle \bar{Y}_l^m \rangle_L$ and $\langle \bar{Y}_l^{m'} \rangle_M$ are the order parameters of the LS_{rep} and mesogen in the laboratory frame, respectively. $\langle [D^{\,l}_{m'm}]^* \rangle_L$ are the order parameters for the LS_{rep} in the mesogen frame, which in a general scenario are described by the Wigner matrices. If we assume axisymmetric order for the mesogen ($\langle \bar{Y}^{m' \neq 0}_l \rangle_M = 0$), $\langle [D^{\,l}_{m'm}]^* \rangle_L$ reduces to spherical harmonics $\sqrt{\frac{4\pi}{2l+1}}(-1)^m \langle Y_l^m(\beta,\gamma) \rangle$.

Principal curvatures of paraboloid and twisted paraboloid

Curvature calculation can be found in any differential geometry textbook. For a three-dimensional surface perimetrically described by $\vec{r}(u,v)$, the principal curvatures at point (u,v) are the maximum (k_{max}) and minimum (k_{min}) curvatures that occur along two orthogonal directions (principal directions).

$$\begin{cases} k_{max} = H + \sqrt{H^2 + K} \\ k_{min} = H - \sqrt{H^2 + K} \end{cases} \qquad S(26)$$

H and K are so called mean and Gaussian curvatures, respectively. They are calculated by:

$$\begin{cases} H = \dfrac{(\vec{r_{uu}} \cdot \vec{N})(\vec{r_{vv}} \cdot \vec{N}) - (\vec{r_{uv}} \cdot \vec{N})^2}{(\vec{r_u} \cdot \vec{r_u})(\vec{r_v} \cdot \vec{r_v}) - (\vec{r_u} \cdot \vec{r_v})^2} \\ K = \dfrac{(\vec{r_u} \cdot \vec{r_u})(\vec{r_{vv}} \cdot \vec{N}) + (\vec{r_v} \cdot \vec{r_v})(\vec{r_{uu}} \cdot \vec{N}) - 2(\vec{r_u} \cdot \vec{r_v})(\vec{r_{uv}} \cdot \vec{N})}{2\left[(\vec{r_u} \cdot \vec{r_u})(\vec{r_v} \cdot \vec{r_v}) - (\vec{r_u} \cdot \vec{r_v})^2\right]} \end{cases} \qquad S(27)$$

, where the derivatives are defined by:

$$\begin{cases} \vec{r_u} = \dfrac{\partial \vec{r}}{\partial u} \\ \vec{r_v} = \dfrac{\partial \vec{r}}{\partial v} \\ \vec{r_{uu}} = \dfrac{\partial^2 \vec{r}}{\partial u^2} \\ \vec{r_{vv}} = \dfrac{\partial^2 \vec{r}}{\partial v^2} \\ \vec{r_{uv}} = \dfrac{\partial^2 \vec{r}}{\partial u v} \end{cases} \qquad S(28)$$

$\vec{r_u}$ and $\vec{r_v}$ are the tangent vectors along u and v, respectively. $\vec{N}$ is the normal vector to the surface, given by:

$$\vec{N} = \frac{\vec{r_u} \times \vec{r_v}}{|\vec{r_u} \times \vec{r_v}|} \qquad S(29)$$

The two principal directions are determined by $\lambda = \frac{dv}{du}$, where λ associated with maximum and minimum principal curvatures can be calculated by solving:

$$\begin{cases} \lambda_{max} + \lambda_{min} = -\dfrac{(\vec{r_u} \cdot \vec{r_u})(\vec{r_{vv}} \cdot \vec{N}) - (\vec{r_v} \cdot \vec{r_v})(\vec{r_{uu}} \cdot \vec{N})}{(\vec{r_u} \cdot \vec{r_v})(\vec{r_{vv}} \cdot \vec{N}) - (\vec{r_v} \cdot \vec{r_v})(\vec{r_{uv}} \cdot \vec{N})} \\ \lambda_{max}\,\lambda_{min} = \dfrac{(\vec{r_u} \cdot \vec{r_u})(\vec{r_{uv}} \cdot \vec{N}) - (\vec{r_u} \cdot \vec{r_v})(\vec{r_{uu}} \cdot \vec{N})}{(\vec{r_u} \cdot \vec{r_v})(\vec{r_{vv}} \cdot \vec{N}) - (\vec{r_v} \cdot \vec{r_v})(\vec{r_{uv}} \cdot \vec{N})} \end{cases} \qquad S(30)$$

By these equations, it is straightforward to obtain the principal curvatures and principal directions at the origin for a paraboloid described by Eq (14) or a twisted paraboloid described by Eq (16). In both cases, the principal curvatures are k_x and k_z with corresponding principal directions being X and Z axes, respectively, and the Y axis is the normal vector.

Experimental procedures

RDC and RCSA data of estrone were collected with 5 mg of material dissolved in a mixed solvent with 351 µL $CDCl_3$, 9 µL DMSO-d_6, and 5 µL TMS (tetramethylsilane) absorbed into a 70% PMMA gel with a 0.02% cross-linking ratio. The gel was allowed to swell overnight and then was stretched in a 4.2/3.2 mm stretch tube. See Ref 5a in the main text for details on PMMA gel recipes and specifications on the stretch tubes. RDC and RCSA data for retrorsine were collected with a 7.5 mg sample dissolved in 333 µL $CDCl_3$, 17 µL DMSO-d_6, and 5 µL TMS and absorbed into a 70% PMMA gel stick with 0.02% cross-linking ratio. The swollen gel was stretched in a 4.2/3.0 mm stretch tube. RDC and RCSA data of aquatolide were collected with ca. 3 mg of material dissolved in 360 µL $CDCl_3$ and 25 µL TMS absorbed into a 70% PMMA gel with a 0.01% cross-linking ratio. The swollen gel was stretched in a 4.2/3.2 mm stretch tube. RDC and RCSA data of caulamidine-A were collected with 1.6 mg of material dissolved in 360 µL $CDCl_3$ and 25 µL TMS absorbed into a 70% PMMA gel with a 0.02% cross-linking ratio. The swollen gel was stretched in a 4.2/3.2 mm stretch tube. RCSA data of parthenolide were collected with 7.1mg of the sample dissolved in 350 µL $CDCl_3$ and 5 µL TMS absorbed into a 70% PMMA gel with a 0.02% cross-linking ratio. The swollen gel was stretched in a 4.2/3.0 mm stretch tube.

The one-bond ^{13}C-^{1}H RDCs were measured with the HD-*J*-HSQC experiment[1] for estrone, aquatolide, and caulamidine-A, the F2-coupled CLIP-HSQC experiment[2] for individual –CH RDCs of the methylene groups of aquatolide, and the ^{13}C observed 2D *J*-resolved experiment with and without the BIRD sequence for the isotropic and anisotropic measurements[3], respectively, for retrorsine. Carbon RCSAs were measured using $^{13}C\{^{1}H\}$ experiments for all compounds as described in Ref 5a. The TMS carbon signal was set to 0.00 ppm for referencing. All experiments were performed at 298 K. A Bruker 600 MHz spectrometer equipped with a liquid N_2 Prodigy™ probe was used for estrone; a Bruker 600 MHz spectrometer equipped with a liquid He cryoprobe was used for aquatolide and caulamidine-A; a Bruker

500 MHz spectrometer equipped with a liquid N_2 Prodigy™ probe was used for retrorsine and parthenolide.

Experimental data

Note: methylene (-CH_2) RDCs collected with the HD-*J*-HSQC experiment or ^{13}C observed 2D *J*-resolved experiment are reported as C-H'/H'', representing the average value of the two one-bond CH RDCs; if both one-bond RDCs on a methylene group are measured using the F2-coupled CLIP-HSQC experiment, they are given on two separate lines as C-H' and C-H'', respectively; methyl RDCs are reported as C-H'/H''/H'''.

Estrone

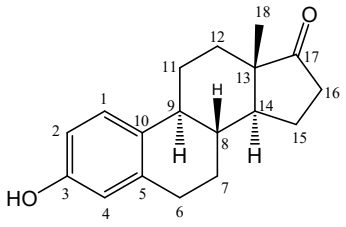

Table S1: RDC data of estrone	
Bond	RDC (Hz)

C1-H1	-16.2
C2-H2	-6.7
C4-H4	-16.3
C9-H9	12.0
C8-H8	13.5
C14-H14	14.0
C6-H6’/6’’	2.2
C16-H16’/16’’	10.0
C11-H11’/11’’	3.8
C15-H15’/15’’	4.1
C7-H7’/7’’	3.6
C12-H12’/12’’	0.9
C18-H18’/18’’/18’’’	-3.8

Table S2: RCSA data of estrone	
Atom	RCSA (Hz)
C17	4.7
C3	1.1
C5	6.0
C10	5.3
C1	7.7
C4	4.4
C2	3.1
C14	-1.3
C13	0.0
C8	-0.5
C16	-1.6
C12	-0.8
C6	-0.4
C7	-0.7
C11	-0.7
C15	-0.5
C18	0.1
C9	-0.1

Retrorsine

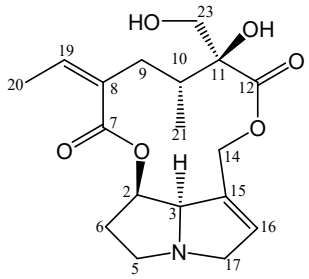

Table S3: RDC data of retrorsine	
Bond	RDC (Hz)
C16-H16	0.2
C19-H19	-0.2
C3-H3	26.2
C2-H2	46.5
C10-H10	16.2
C23-H23’/23’’	2.6
C2-H2’/2’’	7.9
C14-H14’/14’’	16.0
C5-H5’/5’’	-7.1
C9-H9’/9’’	5.5
C6-H6’/6’’	0.5
C20-H20’/20’’/20’’’	8.9
C21-H21’/21’’/21’’’	6.2

Table S4: RCSA data of retrorsine	
Atom	RCSA (Hz)
C12	1.7
C7	2.9
C16	7.9
C19	7.7
C8	6.2
C15	7.0
C11	-1.2
C3	-2.3
C2	-2.6
C23	-1.2
C17	1.5
C14	-2.2
C5	-1.8
C9	-1.3
C10	-1.5
C6	-1.8
C20	-0.9
C21	0.5

Aquatolide

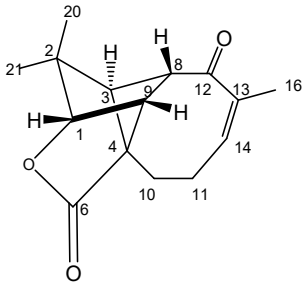

Table S5: RDC data of aquatolide	
Bond	RDC (Hz)
C14-H14	-8.3
C1-H1	11.0
C9-H9	0.7
C8-H8	-0.8
C3-H3	10.7
C10-H10’/10’’	3.8
C11-H11’/11’’	2.5
C11-H11’	-1.2
C11-H11’’	5.2
C16-H16’/16’’/16’’’	0.1
C20-H20’/20’’/20’’’	1.2
C21-H21’/21’’/21’’’	0.9

Table S6: RCSA data of aquatolide	
Atom	RCSA (Hz)
C12	2.1
C6	-1.3
C13	3.0
C14	3.0
C1	-0.4
C4	0.0
C3	0.6
C2	0.2
C11	0.1
C20	-0.1
C21	-0.3

Caulamidine-A

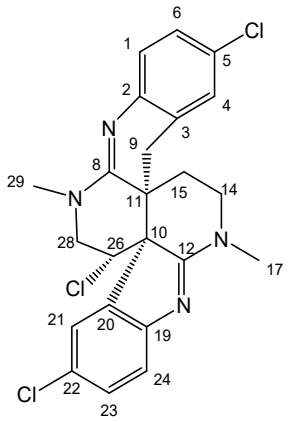

Table S7: RDC data of caulamidine-A	
Bond	RDC (Hz)
C23-H23	29.9
C6-H6	-7.3
C4-H4	-34.5
C1-H1	-39.0
C21-H21	-40.0
C24-H24	-37.6
C26-H26	25.1
C28-H28’/28’’	25.0
C29-H29’/29’’/29’’’	16.5
C17-H17’/17’’/17’’’	18.5

Table S8: RCSA data of caulamidine-A	
Atom	RCSA (Hz)
C12	15.8
C8	13.1
C19	12.5
C2	6.7
C20	2.4
C23	0.5
C6	7.6
C22	10.7
C5	1.9
C4	12.5
C1	12.5
C3	8.6
C21	12.5
C24	12.8
C10	0.5
C26	0.0

C28	-3.6
C14	-3.1
C11	-0.8
C17	-6.8
C29	-5.3
C9	2.1
C15	-1.4

Parthenolide

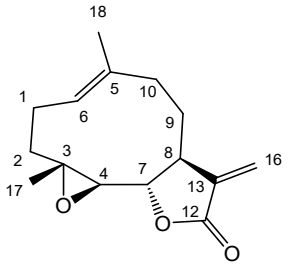

Table S9: RCSA data of parthenolide	
Atom	RCSA (Hz)
C12	15.8
C13	13.8
C5	3.0
C6	0.3
C16	23.6
C7	-4.8
C4	7.1
C3	9.9
C8	0.5
C10	-1.5
C2	2.4
C9	-1.1
C1	-4.6
C17	5.4
C18	2.6

Table S10: Experimental vs predicted data from different prediction models

CMPD	**Cylinder**		**P1**	**P2**	**P3**	**P4**	**P5**	**P6**	**TP1**	**TP2**	**TP3**	**TP4**
1	**exp**	**pred**	**pred**	**pred**	**pred**	**pred**	**pred**	**pred**	**pred**	**pred**	**pred**	**pred**
	-17.7	-5.6	-13.0	-14.9	-18.0	-17.6	-18.8	-19.5	-13.0	-15.4	-18.0	-18.5

	-17.34	-5.6	-12.8	-14.7	-17.8	-17.4	-18.5	-19.3	-12.8	-15.2	-17.8	-18.2
	17.46	16.1	18.8	19.5	17.2	17.6	16.4	15.6	18.4	19.7	17.2	16.7
	5.24	2.0	2.6	6.9	6.4	4.6	6.6	8.0	4.1	7.7	6.2	7.5
	8.95	9.0	9.4	13.2	13.7	11.4	13.9	15.2	11.6	13.5	13.6	15.4
	0.53	-2.3	-2.4	1.5	0.0	-1.2	0.2	1.4	-1.4	2.4	-0.2	0.7
	15.32	13.6	17.5	17.3	16.2	17.0	15.6	14.7	16.8	17.4	16.2	15.4
	-10.57	-10.3	-10.5	-12.7	-9.1	-9.1	-8.3	-7.9	-13.1	-12.3	-8.9	-8.2
	-10.36	-13.4	-11.7	-13.7	-9.0	-8.9	-7.9	-7.1	-14.7	-13.1	-8.7	-8.0
	-8.25	-19.0	-16.4	-15.7	-13.4	-12.9	-12.2	-11.3	-16.8	-15.2	-13.4	-13.7
	5.13	8.9	7.6	9.7	8.5	7.3	8.2	8.5	10.1	9.3	8.3	9.0
	-3.27	-1.5	-3.1	-2.1	-3.0	-3.4	-3.0	-2.9	-1.4	-2.4	-3.1	-3.1
	2.74	9.3	7.2	8.8	6.2	5.3	5.5	5.5	7.8	9.0	6.1	6.6
	7.55	7.6	9.4	11.0	11.6	10.7	11.7	12.2	9.9	11.3	11.6	12.4
	-5.69	-2.3	-3.9	-4.1	-4.7	-4.8	-4.8	-4.6	-5.4	-3.5	-4.6	-4.2
	-4.25	1.1	0.0	-1.8	-0.9	-0.8	-1.0	-1.4	-0.3	-2.3	-0.8	-0.8
	10.5	8.1	10.1	11.0	10.9	10.6	10.8	10.7	10.7	11.0	10.9	11.0
	9.2	9.5	9.7	10.7	9.0	8.8	8.5	8.2	10.9	10.4	8.9	8.8
	9.1	8.2	9.7	10.6	10.2	9.9	10.0	9.9	10.3	10.6	10.2	10.3
	6.6	7.1	7.1	7.9	6.5	6.3	6.0	5.8	8.2	7.6	6.4	6.2
	7.7	8.6	8.9	9.4	8.6	8.3	8.2	7.9	9.5	9.3	8.5	8.6
	-0.1	-0.8	-0.8	-0.7	-0.7	-0.7	-0.6	-0.6	-0.7	-0.7	-0.7	-0.7
	0.2	-0.4	-0.6	-0.3	-0.3	-0.5	-0.3	-0.2	-0.3	-0.3	-0.4	-0.3
	6.2	6.1	5.8	6.9	5.9	5.4	5.6	5.6	7.2	6.6	5.8	5.9
	-1	-2.2	-1.9	-2.1	-1.6	-1.5	-1.5	-1.4	-2.1	-2.1	-1.6	-1.7
	0.2	0.0	0.1	0.2	0.2	0.1	0.2	0.2	0.2	0.2	0.1	0.1
	0.4	0.7	0.6	0.8	0.7	0.6	0.6	0.6	0.8	0.7	0.6	0.6
	-1.8	-1.7	-2.1	-2.4	-2.4	-2.3	-2.4	-2.5	-2.2	-2.4	-2.4	-2.5
	1.4	0.8	1.0	1.4	1.1	1.0	1.0	1.1	1.0	1.5	1.0	1.1
	2.8	2.7	2.8	3.1	2.9	2.8	2.8	2.7	3.4	3.0	2.9	2.8
	3.2	1.2	2.6	1.6	2.9	3.2	3.0	2.8	2.5	1.3	2.9	2.7
	-0.5	-2.1	-1.8	-2.1	-1.8	-1.6	-1.8	-1.8	-1.8	-2.2	-1.8	-2.1
	5.5	2.8	4.7	4.2	5.3	5.6	5.4	5.2	5.1	3.8	5.3	5.1
	8.9	11.1	11.2	11.7	10.4	10.1	9.9	9.6	11.9	11.5	10.4	10.5
	0	-1.1	-0.7	-0.9	-0.6	-0.5	-0.5	-0.6	-0.9	-0.9	-0.6	-0.7
	-1.1	-1.0	-1.1	-1.2	-1.1	-1.1	-1.1	-1.1	-1.3	-1.2	-1.1	-1.1
2	-16.2	-2.8	-8.4	-10.5	-12.9	-14.0	-14.1	-14.9	-7.4	-11.6	-13.2	-13.4
	-6.7	-7.7	-8.8	-8.2	-5.4	-3.6	-3.3	-3.7	-8.5	-8.8	-5.1	-4.4
	-16.3	-3.7	-8.9	-10.7	-13.1	-14.3	-14.3	-15.1	-8.0	-11.7	-13.4	-13.6
	12	21.9	20.6	18.9	16.7	15.6	15.5	14.8	20.9	18.3	16.4	16.3
	13.5	22.6	21.4	19.6	17.2	16.0	16.0	15.2	21.7	18.6	16.9	16.7
	14	22.5	21.1	19.5	16.3	15.2	15.2	14.3	21.8	17.9	16.1	15.7
	-3.8	-6.7	-6.6	-5.9	-5.3	-5.1	-5.1	-4.9	-6.5	-5.6	-5.3	-5.2
	2.2	10.8	10.2	7.8	6.5	6.2	5.9	5.5	9.5	6.7	6.3	6.2

	10	6.9	9.1	9.4	9.3	9.5	9.5	9.6	8.8	9.2	9.4	9.3
	3.8	10.9	9.4	8.6	7.5	7.6	7.6	6.9	10.0	7.1	7.5	7.5
	4.1	14.3	12.0	9.1	8.2	7.8	7.6	6.8	11.6	8.2	7.9	8.1
	3.6	9.1	8.3	7.5	6.9	7.3	7.4	6.7	8.6	5.9	6.9	7.0
	0.9	11.3	9.5	6.8	6.1	5.6	5.3	4.8	8.9	6.5	5.8	5.9
	4.7	6.1	6.8	6.2	5.5	5.3	5.2	5.2	6.6	5.8	5.4	5.3
	1.1	8.1	7.5	6.1	5.6	5.6	5.5	5.1	7.2	5.4	5.5	5.6
	6	7.9	8.4	7.5	6.8	6.5	6.4	6.3	8.0	7.2	6.7	6.6
	5.3	9.2	8.8	7.4	7.0	7.0	6.8	6.5	8.4	6.8	6.9	6.9
	7.7	6.3	7.5	7.1	7.2	7.3	7.3	7.3	7.0	7.0	7.2	7.2
	4.4	4.7	5.6	5.3	5.4	5.5	5.5	5.5	5.2	5.3	5.4	5.4
	3.1	5.1	5.3	4.8	4.1	3.8	3.7	3.7	5.1	4.7	4.0	3.9
	-1.3	-1.3	-1.2	-1.0	-0.9	-0.9	-0.8	-0.8	-1.1	-0.9	-0.9	-0.9
	0	-0.7	-0.4	-0.2	-0.1	0.0	0.0	0.1	-0.4	-0.1	0.0	0.0
	-0.5	-0.1	-0.1	0.0	0.0	-0.1	0.0	0.0	-0.1	0.0	0.0	0.0
	-1.6	-0.9	-1.2	-1.2	-1.2	-1.1	-1.1	-1.2	-1.1	-1.2	-1.2	-1.1
	-0.8	0.1	0.0	0.0	0.0	0.1	0.1	0.0	0.1	-0.1	0.0	0.0
	-0.4	-1.3	-1.1	-0.9	-0.7	-0.6	-0.6	-0.5	-1.1	-0.7	-0.7	-0.6
	-0.7	0.0	-0.1	-0.2	-0.2	-0.2	-0.2	-0.2	-0.1	-0.2	-0.2	-0.2
	-0.7	-0.7	-0.6	-0.6	-0.5	-0.5	-0.5	-0.4	-0.7	-0.5	-0.5	-0.4
	-0.5	-1.2	-1.1	-0.8	-0.7	-0.6	-0.6	-0.5	-1.0	-0.7	-0.6	-0.6
	0.1	1.2	1.1	0.9	0.8	0.7	0.7	0.7	1.1	0.8	0.7	0.7
	-0.1	0.3	0.3	0.3	0.4	0.4	0.4	0.4	0.3	0.3	0.4	0.4
3	-0.17	19.0	13.6	5.8	7.2	7.9	3.8	2.6	9.7	4.8	7.5	-2.9
	26.24	41.7	34.8	30.1	30.0	31.0	27.6	27.8	38.2	29.6	31.3	25.1
	46.51	48.8	49.7	49.5	47.7	47.3	46.9	46.9	49.7	48.6	48.6	47.0
	16.16	44.7	36.6	28.3	29.6	30.2	24.6	23.2	33.7	27.8	29.8	17.6
	8.87	8.3	9.2	8.4	8.6	9.2	9.4	9.5	8.9	7.7	9.2	8.5
	6.19	8.4	5.8	5.8	4.4	3.6	2.5	2.4	7.2	6.3	4.3	3.7
	2.63	10.4	10.5	6.1	9.0	10.6	9.5	8.9	6.6	5.0	9.3	3.9
	7.88	0.9	2.9	3.3	5.0	6.6	8.0	8.7	4.3	2.7	5.7	7.3
	16.01	28.5	23.1	20.4	21.8	22.1	18.8	18.2	22.8	21.3	21.2	16.0
	-7.13	-1.7	-2.3	-4.2	-5.9	-6.3	-6.7	-6.7	-2.3	-5.0	-5.1	-6.6
	5.51	7.3	8.2	5.0	8.9	11.1	10.7	10.5	5.3	4.1	9.1	5.4
	0.51	3.4	0.4	-1.5	1.1	2.6	1.2	1.3	1.5	-1.2	1.0	-1.3
	1.7	-3.3	-2.9	-1.1	-2.0	-2.5	-2.0	-1.7	-1.7	-0.7	-2.2	0.1
	2.9	3.9	3.2	3.8	2.4	1.5	1.3	1.2	3.7	4.0	2.3	2.6
	7.9	6.0	6.3	5.6	6.8	7.7	7.8	8.0	6.5	5.2	7.1	6.5
	7.7	0.7	3.0	4.6	4.2	4.3	5.6	5.9	3.6	4.4	4.5	6.8
	6.2	1.1	3.0	4.3	4.2	4.3	5.5	5.8	3.7	4.0	4.4	6.4
	7	4.3	5.1	4.6	5.9	7.0	7.3	7.5	5.1	4.2	6.3	6.0
	-1.2	-0.9	-1.3	-1.3	-1.5	-1.6	-1.7	-1.7	-1.0	-1.2	-1.5	-1.5
	-2.3	-3.2	-2.7	-2.1	-2.5	-2.8	-2.5	-2.5	-2.7	-2.1	-2.6	-1.8

	-2.6	-2.2	-2.3	-2.4	-2.5	-2.4	-2.4	-2.4	-2.2	-2.5	-2.4	-2.4
	-1.2	-2.4	-2.5	-2.1	-2.2	-2.3	-2.2	-2.2	-2.2	-1.9	-2.3	-1.7
	1.5	3.0	2.3	1.8	2.0	1.9	1.4	1.2	1.9	2.0	1.8	1.0
	-2.2	-4.8	-4.0	-3.7	-3.6	-3.4	-2.9	-2.8	-3.9	-3.9	-3.5	-2.8
	-1.8	-2.6	-2.9	-2.3	-2.3	-2.3	-2.3	-2.2	-2.4	-2.1	-2.4	-1.8
	-1.3	-1.6	-1.6	-1.4	-1.6	-1.8	-1.7	-1.7	-1.5	-1.4	-1.7	-1.4
	-1.5	-1.5	-1.7	-1.5	-1.6	-1.8	-1.8	-1.8	-1.5	-1.4	-1.7	-1.5
	-1.8	-2.0	-1.7	-1.3	-1.6	-1.8	-1.6	-1.6	-1.6	-1.2	-1.6	-1.1
	-0.9	-1.3	-1.3	-1.1	-1.2	-1.4	-1.3	-1.4	-1.3	-1.0	-1.3	-1.1
	0.5	-0.6	-0.3	-0.3	-0.2	-0.1	0.0	0.1	-0.4	-0.3	-0.1	0.0
4	-8.3	-6.9	-6.8	-6.8	-7.8	-8.0	-7.7	-7.5	-7.2	-7.3	-7.7	-8.1
	11	8.9	10.2	9.4	9.8	9.6	10.2	9.8	9.5	9.3	9.9	9.9
	0.7	2.1	1.0	1.5	-0.1	-0.5	0.2	0.6	0.9	1.1	-0.1	-0.6
	-0.8	-0.4	-2.9	-2.0	-1.2	-1.1	-0.4	-0.7	-2.3	-1.1	-1.4	-1.1
	10.7	12.4	12.5	12.5	11.5	11.3	11.6	11.8	12.1	12.0	11.6	11.2
	-1.2	0.0	0.7	0.1	1.0	1.0	1.5	1.0	-0.1	0.3	1.0	1.1
	5.2	7.8	8.2	8.3	8.0	8.2	7.3	7.6	7.9	7.9	8.0	7.7
	0.1	2.0	2.0	2.0	1.8	1.8	1.9	1.9	1.6	1.9	1.9	1.7
	1.2	0.4	1.2	0.9	0.7	0.7	0.5	0.6	1.1	0.6	0.8	0.7
	0.9	2.0	1.9	1.9	1.9	2.0	2.0	1.9	1.6	1.9	1.9	1.8
	3.8	2.7	1.8	2.3	2.5	2.6	2.4	2.5	2.5	2.6	2.4	2.6
	2.5	3.9	4.4	4.2	4.5	4.6	4.4	4.3	3.9	4.1	4.5	4.4
	2.1	1.7	0.9	1.1	1.3	1.3	1.6	1.5	1.4	1.5	1.3	1.5
	-1.3	-0.9	-1.8	-1.4	-1.6	-1.7	-1.5	-1.4	-1.5	-1.3	-1.7	-1.7
	3	3.2	3.4	3.3	3.5	3.5	3.5	3.4	3.2	3.3	3.5	3.5
	3	3.0	3.3	3.2	3.4	3.5	3.4	3.3	3.1	3.2	3.4	3.5
	-0.4	-0.3	-0.5	-0.4	-0.4	-0.3	-0.4	-0.4	-0.4	-0.3	-0.4	-0.4
	0	-0.5	-0.3	-0.4	-0.4	-0.4	-0.5	-0.5	-0.4	-0.5	-0.4	-0.4
	0.6	0.5	0.5	0.5	0.4	0.4	0.4	0.4	0.4	0.4	0.4	0.4
	0.2	-0.1	-0.1	-0.1	-0.1	-0.1	-0.1	-0.1	-0.1	-0.1	-0.1	-0.1
	0.1	-0.3	-0.1	-0.2	-0.2	-0.2	-0.2	-0.2	-0.1	-0.2	-0.2	-0.2
	-0.1	-0.2	-0.4	-0.3	-0.3	-0.2	-0.2	-0.2	-0.3	-0.2	-0.3	-0.3
	-0.3	-0.6	-0.5	-0.6	-0.6	-0.6	-0.6	-0.6	-0.5	-0.6	-0.6	-0.5
5	29.9	17.3	14.4	14.2	11.8	10.9	12.4	13.6	13.6	15.0	12.7	14.8
	-7.3	-40.2	-19.3	-22.2	-16.7	-12.1	-11.0	-12.4	-20.3	-22.0	-15.7	-8.0
	-34.5	-4.7	-33.7	-31.4	-35.5	-38.8	-39.0	-37.7	-34.1	-31.0	-35.8	-39.1
	-39	-4.6	-33.7	-31.3	-35.4	-38.7	-38.9	-37.6	-34.1	-30.8	-35.7	-39.1
	-40	-20.3	-36.4	-37.3	-39.2	-40.5	-40.4	-40.4	-42.6	-35.8	-39.1	-38.2
	-37.6	-18.9	-36.8	-37.3	-39.6	-41.1	-41.0	-40.8	-42.3	-36.0	-39.4	-38.9
	25.1	29.7	33.1	32.6	30.3	28.8	28.9	29.1	27.3	33.9	30.5	30.8
	16.5	3.4	9.7	9.0	9.7	10.5	10.7	10.6	11.1	8.6	9.9	10.3
	18.5	3.7	7.6	7.3	7.7	8.3	8.6	8.7	10.2	6.7	7.8	7.9
	25	22.3	18.6	18.3	16.1	15.0	15.2	15.9	21.7	17.5	16.0	13.2

	15.8	0.9	2.8	1.2	1.2	2.0	2.2	2.1	6.0	0.1	1.3	0.3
	13.1	5.0	8.3	7.3	7.0	7.1	7.3	7.2	6.3	7.7	7.2	8.1
	12.5	-3.3	-0.2	-0.8	0.0	1.0	1.3	1.3	3.9	-1.9	0.1	-0.1
	6.7	9.5	10.5	8.7	7.5	7.0	6.9	6.6	6.5	9.3	7.5	7.4
	2.4	-3.5	-0.4	-0.3	0.8	1.6	1.4	1.2	2.7	-1.2	0.6	0.0
	0.5	-4.0	-0.6	-0.7	0.4	1.2	1.0	0.7	2.3	-1.6	0.2	-0.6
	7.6	13.9	11.7	11.4	9.9	8.8	8.6	8.7	10.1	11.6	9.7	8.1
	10.7	-3.4	-2.4	-2.8	-2.3	-1.6	-1.3	-1.2	1.1	-3.6	-2.2	-2.4
	1.9	4.7	5.0	3.4	2.5	2.1	2.2	1.9	1.4	4.1	2.6	2.9
	12.5	7.2	13.2	11.9	12.0	12.4	12.3	11.9	11.8	12.0	12.1	12.2
	12.5	8.7	13.8	12.7	12.6	12.7	12.7	12.4	12.1	12.9	12.6	12.7
	8.6	13.3	13.0	12.3	11.0	10.1	9.9	9.8	10.8	12.6	10.8	9.7
	12.5	1.3	6.4	6.6	7.7	8.5	8.5	8.4	9.9	5.7	7.6	7.2
	12.8	0.7	6.3	6.2	7.3	8.2	8.2	8.1	9.9	5.2	7.2	6.7
	0.5	0.6	0.8	0.8	0.7	0.7	0.7	0.7	0.7	0.8	0.7	0.7
	0	-3.6	-3.0	-2.7	-2.3	-2.0	-1.8	-1.8	-2.2	-2.8	-2.2	-1.7
	-3.6	-5.1	-3.4	-3.7	-3.1	-2.6	-2.6	-2.7	-3.6	-3.6	-3.0	-2.3
	-3.1	-5.1	-3.4	-3.0	-2.3	-1.9	-1.8	-1.8	-3.6	-2.8	-2.2	-1.0
	-0.8	-0.5	-0.2	0.0	0.1	0.1	0.1	0.1	-0.5	0.1	0.1	0.4
	-6.8	-1.6	-2.7	-2.8	-2.9	-3.1	-3.3	-3.4	-3.9	-2.6	-3.0	-3.0
	-5.3	-0.5	-3.3	-3.3	-3.8	-4.1	-4.2	-4.2	-3.9	-3.2	-3.8	-4.2
	2.1	-1.7	-0.2	-0.4	-0.1	0.3	0.4	0.3	0.4	-0.6	0.0	0.3
	-1.4	1.0	0.0	0.0	-0.2	-0.5	-0.5	-0.5	-0.6	0.2	-0.3	-0.4
6	8	26.5	26.7	24.7	23.7	20.6	20.2	18.8	27.3	26.4	23.7	20.6
	-13	-12.5	-13.4	-13.6	-13.3	-12.7	-12.2	-10.6	-13.2	-14.0	-12.7	-11.9
	29.3	30.8	30.4	30.1	30.6	30.6	30.7	31.1	31.0	29.9	30.2	32.5
	34.2	30.2	30.0	30.2	31.2	32.2	32.1	32.3	30.8	29.8	30.9	33.1
	27.2	33.6	33.6	32.7	33.2	32.7	32.3	31.9	34.7	33.3	33.1	32.8
	-0.8	4.1	4.1	4.1	3.2	2.5	2.7	2.5	3.3	4.2	3.3	2.4
	5.8	5.4	5.1	4.8	5.3	5.6	5.6	5.9	5.6	4.9	5.5	5.6
	-14	-14.6	-14.6	-15.5	-15.0	-15.5	-15.9	-15.9	-13.5	-14.9	-15.1	-15.1
	4.4	8.7	9.4	9.8	8.3	7.3	7.4	6.1	8.0	10.0	8.3	6.2
7	42.5	40.2	42.1	41.9	41.8	40.5	40.9	40.6	41.4	42.0	41.8	41.2
	24.8	22.6	28.3	26.9	25.8	23.6	23.6	22.5	30.5	28.2	26.3	23.7
	38.2	33.4	37.5	36.8	36.9	36.2	36.0	35.5	38.0	37.5	37.2	36.2
	26.6	33.6	33.1	33.1	32.4	30.3	31.2	31.0	31.8	32.8	32.3	31.6
	43.5	35.1	38.9	39.0	40.4	42.0	41.2	41.3	38.1	39.1	40.5	41.5
	29.4	28.2	34.5	32.9	31.3	28.2	28.4	27.2	36.3	34.2	31.7	28.6
	31.1	35.6	36.4	35.6	33.1	28.1	29.7	28.6	36.4	35.8	33.1	30.1
	39	37.9	41.4	40.7	40.0	38.0	38.4	37.6	41.8	41.3	40.2	38.6
	-0.4	0.5	-0.4	-0.4	-0.7	-1.2	-0.9	-0.9	-0.7	-0.5	-0.7	-0.9
	-0.8	-1.3	-1.2	-1.4	-1.8	-2.4	-2.3	-2.5	-0.7	-1.2	-1.7	-2.3
	43.2	36.1	38.8	39.0	40.6	42.3	41.7	41.8	38.3	39.1	40.8	41.8

	-0.6	1.6	0.8	0.4	0.0	-1.3	-0.9	-0.9	0.6	0.4	-0.1	-0.9
	-1.6	-4.9	-3.0	-3.2	-3.3	-2.8	-3.4	-3.3	-3.3	-3.1	-3.3	-3.3
	2.6	-0.8	2.0	1.9	1.5	1.9	1.4	1.3	1.6	2.0	1.5	1.6
	1.4	0.5	0.6	0.7	0.7	0.9	0.8	0.9	0.4	0.6	0.7	0.9
	-1	-1.6	-0.8	-0.8	-0.9	-0.7	-0.9	-0.9	-0.7	-0.8	-0.9	-0.9
	0	-1.7	-1.3	-1.3	-1.3	-1.2	-1.3	-1.3	-1.3	-1.3	-1.3	-1.3
8	-0.1	0.1	-0.4	-0.4	-0.4	-0.4	-0.4	-0.3	0.3	-0.3	-0.4	-0.6
	-0.2	-0.3	-0.2	-0.2	-0.2	-0.2	-0.2	-0.2	-0.4	-0.3	-0.2	-0.2
	-2.4	-1.7	-1.7	-1.7	-1.9	-2.0	-2.0	-2.0	-1.9	-1.7	-1.9	-1.9
	-0.8	-0.9	-0.8	-0.8	-0.8	-0.7	-0.7	-0.7	-0.8	-0.8	-0.8	-0.8
	-0.4	-0.7	-0.7	-0.7	-0.7	-0.7	-0.7	-0.7	-0.7	-0.8	-0.7	-0.7
	-0.8	-0.6	-0.5	-0.5	-0.5	-0.5	-0.5	-0.5	-0.7	-0.4	-0.5	-0.4
	-1.3	-1.0	-0.9	-0.9	-1.0	-1.0	-1.0	-1.0	-1.0	-1.0	-1.0	-1.0
	-3.1	-2.9	-2.7	-2.7	-2.8	-2.9	-2.9	-2.9	-3.1	-2.8	-2.8	-2.8
	0.6	0.2	0.5	0.5	0.7	0.7	0.7	0.6	0.3	0.6	0.6	0.6
	1	1.2	1.4	1.4	1.3	1.2	1.2	1.2	1.0	1.3	1.3	1.3
9	-27	-5.9	2.7	-1.5	-1.7	-0.5	-1.0	-3.9	5.2	-1.8	-1.0	-3.5
	85	80.0	76.1	82.4	82.9	81.0	82.7	83.7	78.8	81.1	82.7	81.9
	7	-12.6	-10.1	-12.9	-9.0	-5.9	-7.5	-7.4	-18.3	-10.7	-8.8	-8.6
	98	80.1	78.6	83.2	86.0	86.2	87.7	87.1	79.1	82.4	86.3	86.0
	97	78.0	74.6	80.7	81.3	79.5	81.2	82.2	77.0	79.4	81.1	80.3
	81	88.2	85.6	90.4	91.4	90.5	92.5	91.4	88.3	88.9	91.6	90.8
	89	85.9	82.0	88.1	88.5	86.7	88.7	89.0	84.8	86.6	88.4	87.6
	-34	-30.8	-48.6	-42.2	-43.6	-45.5	-42.6	-41.9	-43.2	-44.3	-43.8	-35.0
	-34	-47.8	-36.3	-42.0	-42.7	-41.6	-43.5	-44.6	-34.2	-41.4	-42.3	-45.2
	-38	-33.5	-50.4	-45.6	-44.6	-44.5	-41.7	-42.5	-47.7	-47.1	-44.4	-34.6
10	15.8	4.4	6.6	8.6	12.6	17.5	16.5	17.6	9.5	9.6	13.3	13.5
	13.8	16.1	16.6	16.3	15.8	15.8	16.2	16.4	16.9	16.1	15.9	16.6
	3	0.3	1.1	1.9	6.0	7.2	5.0	5.5	-0.5	1.6	5.5	4.0
	0.3	-1.8	-1.2	-1.1	1.6	1.9	0.3	0.9	-2.7	-1.9	1.1	0.1
	23.6	23.4	23.0	23.1	23.0	23.2	23.1	23.2	23.6	23.2	23.1	23.0
	-4.8	-5.0	-5.4	-5.3	-5.4	-5.2	-5.3	-5.2	-4.8	-5.2	-5.3	-5.4
	7.1	4.3	5.3	5.3	6.7	7.3	6.7	7.2	4.9	5.0	6.6	6.6
	9.9	6.4	6.5	6.5	7.9	8.4	7.3	8.0	6.3	6.0	7.7	7.1
	0.5	-0.4	-0.6	-0.4	-0.4	-0.2	-0.3	-0.3	-0.4	-0.3	-0.3	-0.5
	-1.5	-1.5	-1.4	-1.4	-1.7	-1.7	-1.5	-1.6	-1.4	-1.3	-1.6	-1.4
	2.4	0.6	1.5	1.8	2.8	3.6	3.5	3.7	1.6	1.8	2.8	3.1
	-1.1	-2.4	-2.3	-2.4	-2.4	-2.2	-2.3	-2.0	-2.0	-2.6	-2.3	-2.2
	-4.6	-2.6	-2.7	-2.8	-3.1	-3.7	-3.5	-3.8	-3.3	-2.9	-3.2	-3.2
	5.4	3.5	3.7	4.1	4.6	5.4	5.2	5.4	4.3	4.3	4.8	4.7
	2.6	1.0	0.4	0.7	0.6	0.9	0.7	0.7	1.0	0.9	0.7	0.4
11	29.5	28.8	30.0	30.8	30.3	29.4	28.5	28.3	29.6	31.3	30.5	29.2
	-6.4	-7.4	-15.7	-19.4	-16.4	-16.7	-14.3	-15.5	-15.7	-18.8	-16.6	-13.8

	-20.6	-21.4	-14.1	-13.9	-20.1	-21.1	-22.1	-22.4	-12.2	-15.7	-19.8	-21.4
	-10.1	-17.5	-20.3	-19.1	-17.5	-16.9	-16.3	-14.8	-20.6	-18.7	-17.5	-14.8
	-9.4	-7.3	-15.8	-19.5	-16.4	-16.6	-14.2	-15.4	-15.9	-18.8	-16.6	-13.7
	30.5	30.2	31.3	32.1	31.5	30.4	29.5	29.2	31.0	32.7	31.7	30.3
	32.2	31.4	32.5	33.3	32.7	31.7	30.7	30.4	32.2	34.0	33.0	31.4
	-4.2	-3.5	0.4	0.3	0.5	1.8	1.3	1.0	0.1	-0.6	0.2	-2.3
	30.3	30.6	31.8	32.6	32.1	31.1	30.2	29.9	31.4	33.2	32.3	30.8
	7.6	12.5	9.1	8.9	11.0	11.0	11.3	11.2	8.5	10.0	11.0	11.6
	10.4	13.6	9.7	9.0	10.7	10.2	10.7	10.4	9.3	10.0	10.7	11.7
	9.8	6.0	9.0	10.4	8.4	7.9	6.9	7.3	9.3	10.3	8.7	7.9
	7.9	13.6	9.5	8.8	10.6	10.1	10.7	10.4	9.1	9.8	10.6	11.6
	9.3	13.1	9.0	8.2	10.1	9.6	10.2	9.9	8.6	9.2	10.1	11.1
12	-28.3	-29.4	-29.8	-26.2	-26.7	-30.0	-28.9	-28.2	-25.7	-26.6	-27.2	-25.4
	1.6	-13.9	-26.1	-24.3	-20.0	-16.6	-16.7	-15.2	-21.0	-20.8	-20.0	-20.4
	36.5	37.7	37.3	40.9	40.4	37.1	38.2	38.9	40.7	40.5	39.9	40.6
	38.8	37.4	36.4	40.4	39.2	35.5	36.8	37.7	41.4	39.3	38.7	41.7
	32.2	28.9	28.5	30.0	30.1	27.9	28.5	29.1	33.1	30.8	29.4	31.7
	-3.8	3.5	6.7	6.6	5.3	4.1	4.3	3.9	5.5	5.4	5.3	5.6
	-10.7	-11.8	-11.9	-13.2	-12.9	-11.8	-12.2	-12.3	-12.4	-12.8	-12.8	-12.6
	4.8	-0.8	-4.1	-3.7	-3.0	-2.5	-2.5	-1.9	-0.9	-2.9	-3.1	-1.0
	20.4	22.8	26.4	25.5	23.2	22.4	22.4	21.9	24.6	23.2	23.4	25.2
	20.1	15.7	10.1	13.0	14.4	14.1	14.6	15.7	14.1	14.1	14.2	14.5
13	12	12.2	12.4	12.3	12.3	12.4	12.3	12.3	12.3	12.2	12.3	12.3
	-2.4	-1.0	-1.6	-1.6	-1.5	-1.1	-1.5	-1.1	-2.5	-2.3	-1.7	-0.7
	0.5	0.2	0.2	0.3	0.4	0.2	0.3	0.3	0.7	0.6	0.4	0.2
	-3.4	-3.2	-3.0	-3.1	-3.1	-3.0	-3.1	-3.1	-3.1	-3.2	-3.1	-3.1
	5.6	6.3	6.5	6.2	6.1	6.5	6.2	6.3	5.6	5.8	6.0	6.4
	2.7	3.6	3.2	3.6	3.9	4.2	3.8	3.9	4.8	3.6	4.0	4.1
	2.8	3.1	3.7	3.5	3.2	2.8	3.3	3.1	2.8	3.8	3.3	2.7
	4.6	4.7	3.9	4.4	4.4	4.2	4.4	4.6	3.9	4.3	4.4	4.8
	0.2	-0.1	-0.1	-0.1	-0.2	-0.2	-0.2	-0.2	-0.3	-0.1	-0.2	-0.2
14	23.8	20.7	24.1	22.8	23.7	23.4	23.4	23.3	23.1	21.5	22.6	23.9
	21.4	21.7	25.4	24.2	25.2	24.9	24.9	24.9	24.5	22.9	24.0	25.0
	20.8	19.9	23.0	22.0	22.8	22.7	22.6	22.5	22.3	20.7	21.9	22.9
	10.3	9.8	12.3	11.3	11.4	9.8	10.6	11.3	12.9	11.7	10.1	9.7
	12	11.7	14.8	13.8	13.7	11.9	12.7	13.4	15.0	14.0	12.2	11.6
	2.4	3.4	4.3	4.0	4.0	3.7	3.8	3.9	3.1	3.6	3.6	4.1
	3.9	3.4	4.0	3.9	4.5	4.4	4.6	4.8	4.5	4.0	4.3	4.2
	4.7	3.9	4.5	4.3	3.8	3.5	3.5	3.5	4.3	4.0	3.5	3.6
	7.6	7.9	9.8	9.4	10.7	10.6	10.8	11.0	9.1	9.1	10.1	10.2
	8.5	9.0	10.7	10.0	9.8	9.5	9.5	9.4	8.9	9.0	9.2	10.2
	12.5	11.6	13.7	12.9	13.2	12.5	12.8	13.0	14.1	12.7	12.4	12.5
	2.4	4.6	5.3	5.1	6.3	6.8	6.8	6.8	5.4	4.9	6.3	6.6

15	-20.8	-7.6	-18.7	-24.2	-20.8	-19.6	-19.5	-19.8	-19.4	-23.0	-21.0	-19.1
	-19.8	-28.2	-23.9	-18.2	-22.3	-22.2	-22.8	-22.0	-24.6	-20.4	-22.3	-22.0
	-10.6	-15.4	-15.9	-14.6	-16.9	-17.9	-16.1	-17.4	-12.1	-15.8	-16.9	-19.0
	-20.4	-7.8	-18.9	-24.5	-21.1	-19.9	-19.9	-20.1	-19.8	-23.4	-21.3	-19.4
	21.6	30.5	32.6	34.9	34.6	32.5	31.6	31.9	33.6	35.9	34.7	33.5
	38.6	31.2	35.5	34.7	37.1	37.2	36.6	37.4	34.8	36.0	37.1	37.4
	5.4	3.9	4.0	4.6	4.8	4.4	4.9	5.0	5.8	4.6	4.8	4.4
	14	14.7	12.2	10.6	13.2	13.3	14.1	14.4	14.5	11.5	13.2	13.5
	12.9	14.5	15.9	15.1	16.3	16.5	15.5	16.0	13.9	16.0	16.3	17.0
	-6	-11.9	-13.8	-12.6	-13.0	-13.2	-11.8	-12.0	-10.4	-13.4	-13.1	-13.4
	7.9	4.1	8.1	12.1	9.8	8.4	8.4	8.5	9.8	11.5	9.9	8.6
	-16.4	-15.0	-12.9	-10.8	-13.8	-14.2	-14.9	-15.3	-14.6	-11.8	-13.8	-14.4
	8.2	14.0	13.7	12.3	13.0	12.7	11.4	11.4	11.2	13.4	13.1	13.2
16	-16.7	-5.1	-14.7	-18.2	-16.4	-14.7	-15.4	-14.7	-13.0	-18.2	-17.0	-18.0
	-10.9	-10.1	-9.0	-9.7	-12.9	-11.8	-12.5	-13.2	-6.9	-9.2	-12.0	-12.0
	-16.7	-21.4	-18.9	-12.8	-17.1	-19.2	-18.6	-18.3	-19.2	-13.0	-17.1	-17.7
	-14.5	-5.0	-14.5	-18.0	-16.3	-14.6	-15.3	-14.6	-12.8	-18.0	-16.9	-17.9
	26.8	22.1	24.6	25.3	26.4	24.3	24.9	25.2	24.3	25.3	26.4	25.5
	8.9	10.2	9.1	8.6	11.9	11.7	12.0	12.8	8.0	8.1	11.4	11.6
	-9.6	-8.1	-8.6	-8.5	-12.0	-12.0	-12.3	-13.0	-6.7	-7.9	-11.5	-12.3
	11.4	10.5	9.6	7.1	7.2	7.5	7.3	6.6	10.4	7.7	7.4	6.9
	11.9	10.0	10.6	10.5	13.0	12.6	12.9	13.3	9.2	10.2	12.6	12.9
	8	3.4	7.3	9.7	7.8	6.2	6.6	6.4	7.3	9.8	8.1	7.7
	-11.7	-10.3	-9.7	-7.1	-7.6	-8.2	-7.9	-7.2	-10.1	-7.6	-7.7	-7.6

The predicted data are rescaled into approximately the same range as the experimental data by a factor of $(exp_{max} - exp_{min})/(pred_{max} - pred_{min})$ to facilitate inspection.

References:

1. L. Castanar, M. Garcia, E. Hellemann, P. Nolis, R. R. Gil and T. Parella, *J Org Chem*, 2016, **81**, 11126-11131.
2. A. Enthart, J. C. Freudenberger, J. Furrer, H. Kessler and B. Luy, *J Magn Reson*, 2008, **192**, 314-322.
3. Y. Z. Liu, R. D. Cohen, G. E. Martin and R. T. Williamson, *J Magn Reson*, 2018, **291**, 63-72.